Journal of Power Sources 185 (2008) 226–232

Contents lists available at ScienceDirect

Journal of Power Sources

journal homepage: www.elsevier.com/locate/jpowsour

Optimization of the polypyrrole-coating parameters for proton exchange membrane fuel cell bipolar plates using the Taguchi method

Yan Wang, Derek O. Northwood*

Department of Mechanical, Automotive, and Materials Engineering, University of Windsor, 401 Sunset Avenue, Windsor, Ontario, Canada N9B 3P4

ARTICLE INFO

Article history:
Received 9 June 2008
Received in revised form 11 July 2008
Accepted 15 July 2008
Available online 25 July 2008

Keywords:
PEMFCs
Bipolar plates
Polypyrrole
Taguchi
Corrosion

ABSTRACT

In order to overcome the high price, weight and volume of non-porous graphite bipolar plates, metallic bipolar plates are being investigated as a substitute material. However, metallic materials can corrode under proton exchange membrane fuel cell (PEMFC) working conditions, leading to a degradation in the performance of the membrane. Previous work had shown that a polypyrrole coating on SS316L can significantly increase the corrosion resistance of the base material. In this study, a Taguchi design of experiment method was used to optimize the process parameters for the polypyrrole coating so as to produce the maximum corrosion resistance. Potentiodynamic and potentiostatic tests were used to determine the corrosion resistance of the polypyrrole-coated SS316L. Scanning electron microscopy (SEM) with energy dispersive X-ray (EDX) was used to characterize the coating thickness and coating appearance. Inductively coupled plasma optical emission spectroscopy (ICP-OES) was used to determine the metal ion concentration in the solution after corrosion. The interfacial contact resistance of SS316L with carbon paper was measured both before and after coating with polypyrrole.

© 2008 Elsevier B.V. All rights reserved.

1. Introduction

With escalating oil prices (about US$140/barrel) and increasing environmental concerns, increasing attention is being paid to fuel cell technology. Proton exchange membrane fuel cells (PEMFCs) are receiving wide attention because of their low operation temperature and fast start-up.

Bipolar plates are one of the most important components in PEMFCs and are designed to accomplish many functions, including: separate the individual cells in the stack; facilitate water management within the cell; carry current away from the cell; distribute the fuel and oxidant in the stack; and facilitate heat management [1]. However, the non-porous graphite bipolar plates account for about 80% of the total weight, 45% of stack cost and almost the whole volume [2]. Therefore, they are one of the major barriers to the more widespread application of PEMFCs.

Currently, two major types of materials, metallic and composite materials, are being researched to substitute for non-porous graphite for the fabrication of bipolar plates for PEMFCs. Both materials have their advantages and disadvantages as bipolar plate materials. Metallic materials have good mechanical stability, electrical conductivity and thermal conductivity and can be recyclable. However, in a PEMFC environment, metals are prone to corrosion and the resulting metal ions can readily migrate to, and poison, the membrane [3,4]. The dissolved metal ions can lower the ionic conductivity of the membrane and, thus, the performance of the PEMFC. Furthermore, any corrosion layer will lower the electrical conductivity of the bipolar plates, and increase the potential loss because of a higher electrical resistance. Hence, in order to be suitable materials of bipolar plates, metals should have both a very high corrosion resistance and high electrical conductivity [5].

Conductive polymers are a new type of material, which have a high redox potential and properties of both metals and plastics. The electrochemical polymerization of a conductive polymer has been used to coat metallic materials in order to fabricate bipolar plate materials [6–8]. In our earlier research [8], we have coated polypyrrole on SS316L surface and it showed that the corrosion resistance was increased about 10 times compared to the bare metal. However, this previous study [8], examined a very limited number of process parameters and there was a need to determine whether the corrosion resistance could be further improved.

In this study, the Taguchi method for design of experiment was used for the optimization of the polypyrrole-coating param-

* Corresponding author. Tel.: +1 519 253 3000x4785; fax: +1 519 973 7007.
E-mail addresses: wang167@uwindsor.ca (Y. Wang), dnorthwo@uwindsor.ca (D.O. Northwood).

0378-7753/$ – see front matter © 2008 Elsevier B.V. All rights reserved.
doi:10.1016/j.jpowsour.2008.07.036

Table 1
Experimental layout using a L9 orthogonal array

Experiment number	Column number			
	A (applied current)	B (time)	C (concentration of polypyrrole)	D (concentration of H_2SO_4)
1	1	1	1	1
2	1	2	2	2
3	1	3	3	3
4	2	1	2	3
5	2	2	3	1
6	2	3	1	2
7	3	1	3	2
8	3	2	1	3
9	3	3	2	1

eters for the PEM fuel cell bipolar plates. A classical optimization method would design experiments that identify all possible combinations for a given set of variables. This approach is called the full factorial design and it takes into account a large number of experiments, which can be costly and time consuming. Taguchi [9] proposed a design of experiment method, which minimizes the number of experiments to a practical level for optimization processes. Taguchi's parameter design has proved to be an effective approach producing high quality products at a relatively low cost. Some initial results from this Taguchi DOE have been reported in Ref. [10].

2. Experimental details

2.1. Taguchi design of experiment

The Taguchi method uses a special of orthogonal arrays to study all the designed factors with a minimum of experiments. Orthogonality means that factors can be evaluated independently of one another; the effect of one factor does not interfere with the estimation of the influence of another factor [9]. Four factors (applied current (A), time (B), the concentration of polypyrrole (C), the concentration of H_2SO_4 (D)) with three levels were selected as shown in Table 1. The factors and levels were used to design a experimental layout using a $L_9(3^4)$ array. The experiments were repeated 3 times in order to ensure reliability. For the applied current, levels of 0.0002 A (1), 0.0005 A (2), 0.001 A (3) were used. For coating time, levels of 10 min (1), 30 min (2), 60 min (3) were used. For the concentration of polypyrrole, levels of 0.05 mol L^{-1} (1), 0.1 mol L^{-1} (2), 0.2 mol L^{-1} (3) were used. For the concentration of H_2SO_4, levels of 0.05 mol L^{-1} (1), 0.1 mol L^{-1} (2), 0.2 mol L^{-1} (3) were used.

2.2. Polypyrrole coating

SS316L was chosen as the base material primarily because of its good corrosion resistance and relatively cheap price. The chemical composition of the SS316L is shown in Table 2. In this study, the galvanostatic method was used to coat polypyrrole on SS316L. In the galvanostatic coating, different currents, coating times, concentrations of polypyrrole and sulphuric acid were utilized to coat the polypyrrole. The electrochemical instrumentation used was a Solartron 1285 potentiostat. A typical three-electrode system was used. SS316L, Pt and saturated calomel electrodes are the working electrode, counter electrode and reference electrode, respectively. The coating temperature was ambient temperature.

Table 2
Chemical composition of SS316L (wt%)

Metal	SS316L
C	0.021
Mn	1.82
P	0.029
S	0.01
Si	0.58
Cr	16.32
Ni	10.54
Mo	2.12
Cu	0.47
N	0.03
Fe	Balance

2.3. SEM

Scanning electron microscopy (SEM) and energy dispersive X-ray analysis (EDX) analysis were used to observe the surface morphologies and analyze the chemical compositions. If only the surface morphology was to be examined, a JEOL JSM-5800LV SEM was used. If both surface morphology and chemical analysis were required, an environmental scanning electron microscope (ESEM) facility equipped with EDX was used [FEI Quanta 200F with a solid state back scattered detector (BSD)].

2.4. Electrochemistry

Both potentiodynamic and potentiostatic tests were used to analyze the corrosion characteristics of the uncoated and coated samples. In the potentiodynamic tests, the initial potential was −0.1 V vs. open circuit potential (OCP), and the final potential was 1.2 V vs. saturated calomel electrode (SCE) and the scan rate was 1 mV s^{-1}. In the potentiostatic tests, at the anode, the applied potential was −0.1 V vs. SCE purged with H_2 and at the cathode, the applied potential was 0.6 V vs. SCE purged with O_2 [11]. The setting time was 10 h with 1 point s^{-1}. Both the potentiodynamic and potentiostatic tests were conducted at 70 °C because PEM fuel cells are generally operated at temperatures between 50 °C and 100 °C [12].

2.5. Metal ion concentration in solution after potentiostatic tests

Inductively coupled plasma optical emission spectrometry (ICP-OES) (IRIS #701776, Thermo Jarrell Ash Corporation) was used to investigate the metal ion concentrations in solution after corrosion. Liquid samples were introduced into the instrument via a Meinhard concentric glass nebulizer (TK-30-K2, JE Meinhard Associates Inc., California, USA) combined with a cyclonic spray chamber. The areosol was then introduced into a radial orientation argon plasma resulting in characteristic emission lines that are simultaneously resolved using argon purged echelle optics and a themostatted charge injection device detector. The total solution volume for ICP-OES is 7 mL.

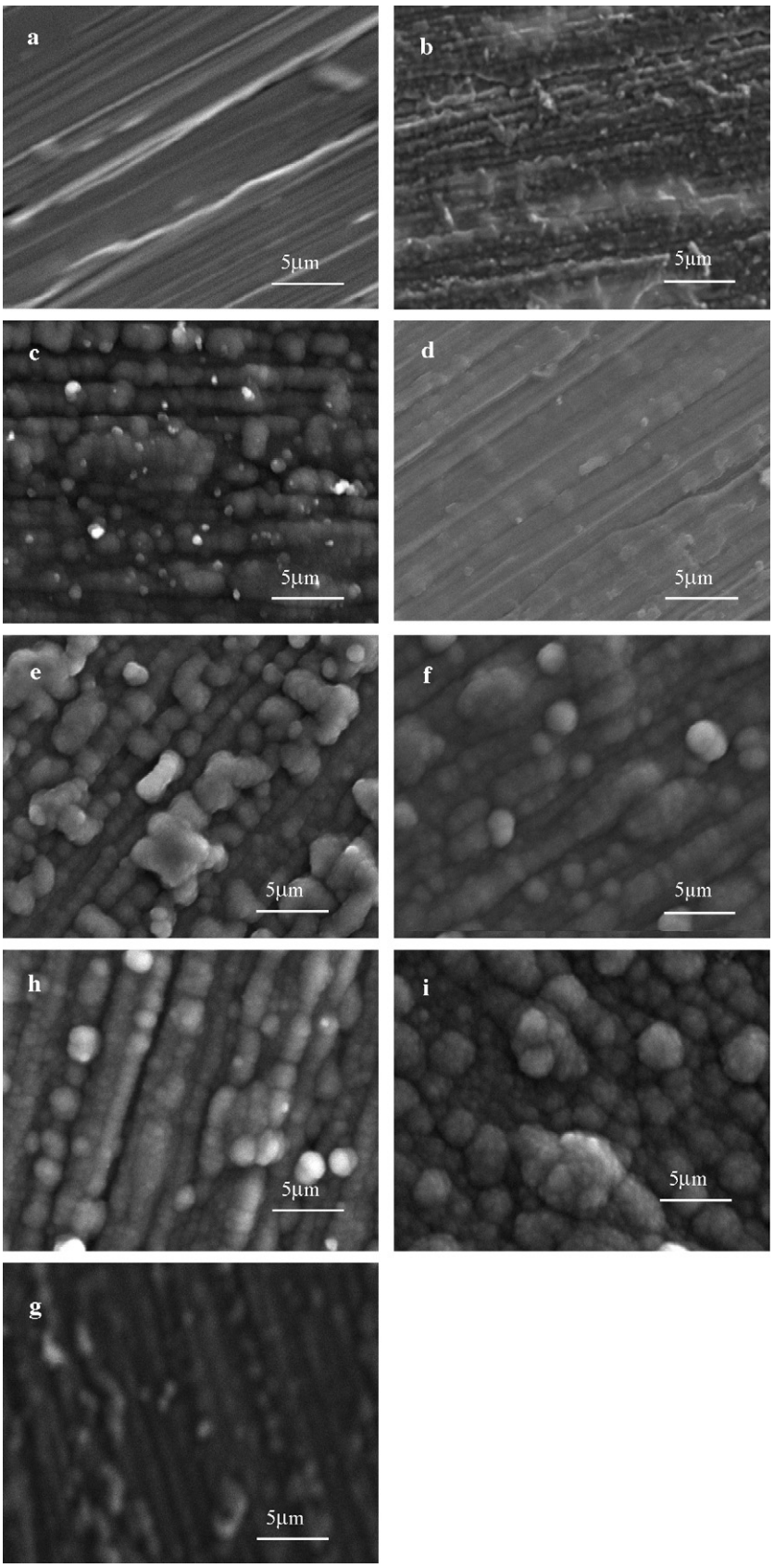

Fig. 1. SEM micrographs of SS316L coated with polypyrrole: (a) experiment 1, (b) experiment 2, (c) experiment 3, (d) experiment 4, (e) experiment 5, (f) experiment 6, (g) experiment 7, (h) experiment 8, (i) experiment 9 (for process parameters, see Table 1).

Table 3
The thickness of polypyrrole coating with different coating conditions

Coating condition	Coating thickness (μm)
1	7 ± 0.5
2	21 ± 0.5
3	46 ± 0.5
4	18 ± 0.5
5	43 ± 0.5
6	50 ± 0.5
7	25 ± 0.5
8	43 ± 0.5
9	54 ± 0.5

2.6. Contact resistance tests

The interfacial contact resistance measurements were made using a standard testing method [13,14]. All interfacial contact resistance measurements were carried out at room temperature. In our setup, two pieces of Toray conductive carbon paper (Fuel Cell Store) were sandwiched between the metal sample and the copper plates. A GW Instel GOM-802 milliohm meter was used to measure the electrical resistance. The compaction force was gradually increased using a Tinus Olsen test machine and the contact resistance was measured.

3. Results and discussion

3.1. SEM of polypyrrole-coated materials

Fig. 1a–i are SEM micrographs of polypyrrole-coated SS316L produced at different process conditions. Two types of polypyrrole structure can be seen. In Fig. 1a, b, d and g, the polypyrrole film is quite thin and the polishing marks from the 240 grit polishing of the SS316L are still visible. In Fig. 1c, e, f, h and i, we can see polypyrrole particles, which are between 1 μm and 3 μm in size. Comparing the particle sizes in the different coatings, it was found that the polypyrrole particle size increased with both increasing coating current and coating time.

From cross-sectional micrographs, we determined the thickness of the polypyrrole coating for different coating conditions, and these are given in Table 3. We can see that the polypyrrole coatings have different thickness with different coating conditions. The thickness of polypyrrole coatings for coating conditions 1, 2, 4, 7 are relatively thin (less than 30 μm) compared to coating conditions 3, 5, 6, 8, 9 (more than 30 μm). Therefore, in general, the coating thickness increased with increased coating time, coating current and polypyrrole concentration.

Our earlier studies [15] have shown that the nucleation and growth behavior of polypyrrole on SS316L could be divided into three stages. The first stage is an incubation period. The second stage is a combination of instantaneous nucleation and two-dimensional growth and instantaneous nucleation and three-dimensional growth. The third stage is a combination of instantaneous nucleation and three-dimensional growth and progressive nucleation and three-dimensional growth.

3.2. Corrosion resistance of polypyrrole coatings

A linear polarization method was used to obtain the polarization resistance of SS316L at 70 °C:

$$R_p = \frac{\beta_a \beta_c}{2.3 i_{corr}(\beta_a + \beta_c)} \quad (1)$$

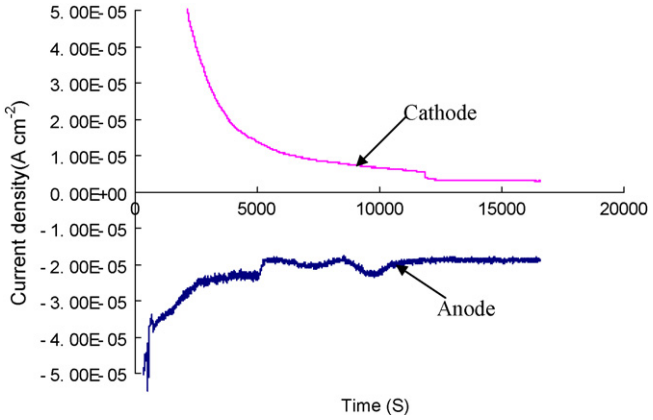

Fig. 2. Potentiostatic curve for polypyrrole-coated SS316L in the simulated anode and cathode environments (condition 5).

where β_a, β_c, i_{corr}, and R_p are the Tafel slopes of the anodic and cathodic reactions, the corrosion current density and polarization resistance, respectively [16].

The corrosion potential increased and the corrosion current density decreased after coating polypyrrole on SS316L: see Table 4. In our earlier studies [17,18], the polarization resistance and corrosion current density of uncoated SS316L were found to be 328 Ω cm^2 and 40 μA cm^{-2} at 70 °C, respectively, for the same test conditions. From the linear polarization data, the polarization resistance for the thin (less than 30 μm) polypyrrole coatings (Fig. 1a, b, d and g) was around 1500 Ω cm^2, which is about 5 times higher than for the uncoated samples. Also, the polarization resistance of relatively thick (more than 30 μm) polypyrrole coating (Fig. 1c, e, f and h) is about 3500 Ω cm^2, which increased the polarization resistance of SS316L by more than 10 times. The polarization resistance and corrosion current density for uncoated SS316L are about 4200 Ω cm^2 and 5 μA cm^{-2} at 20 °C, respectively [17,18]. Therefore, the polarization resistance and corrosion current density for a relatively thick polypyrrole-coated material at high temperature (70 °C) are of the same order as those of the uncoated SS316L at ambient temperature (20 °C).

3.3. Potentiostatic tests with polypyrrole-coating chosen on basis of linear polarization tests

In actual PEMFC working conditions, the anode is at a potential of about −0.1 V vs. SCE and the cathode is at a potential of about 0.6 V vs. SCE. Under these PEMFC conditions, any corrosion that takes place is not the same as the corrosion at OCP. In order to study the corrosion behavior of metallic bipolar plates in actual PEMFC working conditions, potentiostatic tests were conducted at −0.1 V vs. SCE purged with H_2 to simulate the anode working conditions and at 0.6 V vs. SCE purged with O_2 to simulate the cathode working conditions.

Polypyrrole-coated SS316L (condition 5) was chosen for the potentiostatic tests because it had one of the higher corrosion resistances and the coating time required was relatively short (30 min). The total test time for the potentiostatic tests was 10 h for the simulated anode and cathode conditions. However, the software used could only store 16,800 points (about 4.67 h) at 1 point s^{-1} speed. Therefore, Fig. 2 shows only part of the total potentiostatic test curve.

Fig. 2 shows that the corrosion current density is negative in the simulated anode side. However, it is positive in the simulated cathode side. This is because OCP of polypyrrole-coated SS316L is around 0.2 V vs. SCE. The simulated anode and cathode are −0.1 V vs.

Table 4
Polarization resistance of polypyrrole-coated SS316L at 70 °C

Results	No.								
	1	2	3	4	5	6	7	8	9
β_a (V)									
Test 1	0.128	0.179	0.204	0.173	0.067	0.247	0.322	0.159	0.152
Test 2	0.163	0.163	0.141	0.259	0.192	0.265	0.137	0.208	0.163
Test 3	0.185	0.189	0.113	0.192	0.123	0.467	0.178	0.191	0.185
β_c (V)									
Test 1	0.107	0.050	0.025	0.051	0.027	0.021	0.056	0.018	0.023
Test 2	0.126	0.058	0.051	0.050	0.025	0.027	0.063	0.017	0.026
Test 3	0.118	0.049	0.031	0.054	0.027	0.021	0.054	0.018	0.029
E_{corr} (V)									
Test 1	0.129	0.137	0.145	0.142	0.146	0.154	0.158	0.171	0.233
Test 2	0.128	0.129	0.147	0.140	0.145	0.160	0.155	0.179	0.215
Test 3	0.130	0.127	0.142	0.141	0.147	0.168	0.156	0.188	0.222
i_{corr} ($\mu A\,cm^{-2}$)									
Test 1	17.91	13.90	2.78	10.85	2.08	2.72	11.88	2.66	2.38
Test 2	16.93	12.06	2.99	12.53	2.53	2.50	14.72	2.24	2.85
Test 3	20.64	12.83	2.41	11.35	2.67	2.13	10.05	2.29	2.69
R_p ($\Omega\,cm^2$)									
Test 1	1415	1222	3483	1578	4023	3094	1746	2643	3649
Test 2	1825	1542	5446	1454	3801	4261	1275	3050	3421
Test 3	1518	1339	4389	1614	3605	4102	1792	3123	4052

SCE and 0.6 V vs. SCE, respectively. Therefore, the potential of the simulated anode is anodic to the potential of polypyrrole-coated SS316L and the potential of the simulated cathode is cathodic to the potential of polypyrrole-coated SS316L. This negative current density can provide cathodic protection for the metallic bipolar plate material. The negative current arises because of the following reactions [8]:

$$2H^+ + 2e^- \rightarrow H_2 \qquad \text{metalelectrode} \tag{2}$$

$$2H_2O \rightarrow 4H^+ + O_2 + 4e^- \qquad \text{platinumelectrode} \tag{3}$$

3.4. SEM and EDX tests of polypyrrole-coated SS316L after potentiostatic tests

Fig. 3 presents SEM micrographs and associated EDX spectra of the coatings after potentiostatic testing. The polypyrrole coatings were still intact and covered the whole surface after 10-h potentiostatic tests in both the simulated anode and cathode environments. In the EDX spectra, the elemental peaks for C, N, O and S are from the polypyrrole, whereas the Fe, Cr, Ni and Si peaks arise from the SS316L base material since the polypyrrole coating is quite thin.

3.5. ICP-OES tests for coating subjected to potentiostatic testing

In a 'real' PEM fuel cell, metal ions generated from corrosion can migrate to the membrane and levels as low as 5–10 ppm can degrade the membrane performance [19,20]. Therefore, metal ion concentration in solution is a very important parameter for the metallic bipolar plate performance. Metal ion concentrations were determined to find the ion concentration left in the solution after the 10 h potentiostatic tests in the simulated anode and cathode environments.

Table 5 summarizes the metal ion concentrations in the 10 h potentiostatic tests in the simulated anode and cathode conditions for a PEM fuel cell. Comparing the data in Table 5, we find that metal ion concentration at the cathode is much higher than that at the anode for all the elements analysed for both uncoated and polypyrrole-coated samples. Also, comparing the results of uncoated and polypyrrole-coated SS316L, we find that the metal ion concentration in solution for polypyrrole-coated SS316L is only about half that for the uncoated samples. For example, the Fe ion concentrations for uncoated SS316L are 771 $\mu g\,L^{-1}$ or 1246 $\mu g\,L^{-1}$ in the simulated anode and cathode environments, respectively. The Fe ion concentrations for polypyrrole-coated SS316L are 434 $\mu g\,L^{-1}$ or 826 $\mu g\,L^{-1}$ in the simulated anode and cathode environments, respectively. Therefore, based on our research results, metal corrosion is more severe in the cathode environment, which is consistent with the potentiostatic test results. The metal ion concentrations measured in the simulated anode conditions seems at odds with the potentiostatic tests because the negative current should provide cathodic protection for SS316L. The reason why we still get a relatively high metal ion concentration at the anode is that the cathodic protection is only partial and it cannot provide full protection for the SS316L. The applied potential is not negative enough to provide full protection for SS316L. Therefore, SS316L can be corroded in both the anode and cathode environments, and corrosion in the cathode environment is the hot spot.

Table 5
Metal ion concentrations after potentiostatic tests

Environment	Dissolved metal concentration ($\mu g\,L^{-1}$)				Total concentration of metal ions ($\mu g\,L^{-1}$)
	Fe	Cr	Ni	Mn	
Base solution	21	<IDL	<IDL	1	22
Uncoated SS316L at anode side	771	129	81	20	1001
Uncoated SS316L at cathode side	1246	230	180	36	1692
Coated SS316L at anode side	314	59	50	11	434
Coated SS316L at cathode side	656	60	91	19	826

Note: IDL is the identification limit.

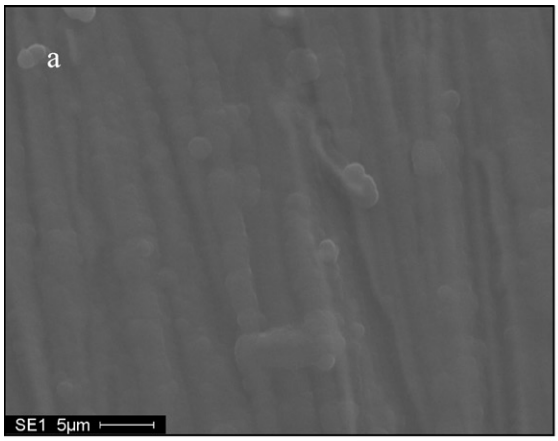

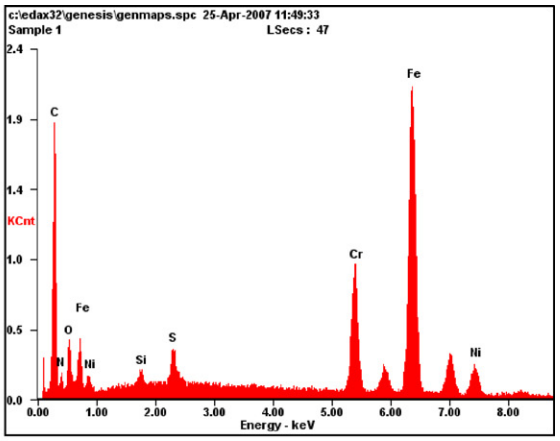

Element	Wt%	At%
CK	47.23	73.15
NK	04.44	05.89
OK	05.36	06.24
SiK	00.30	00.20
SK	00.77	00.44
CrK	07.61	02.72
FeK	29.93	09.97
NiK	04.38	01.39
Matrix	Correction	ZAF

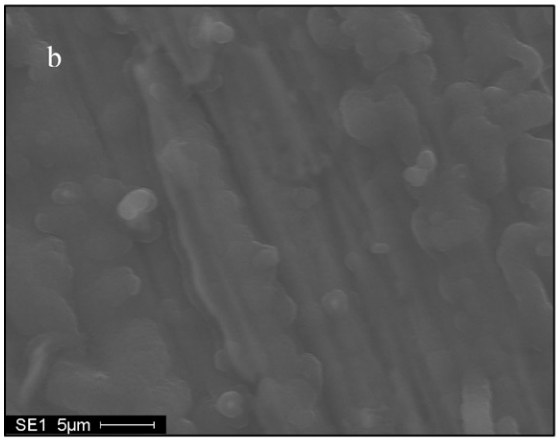

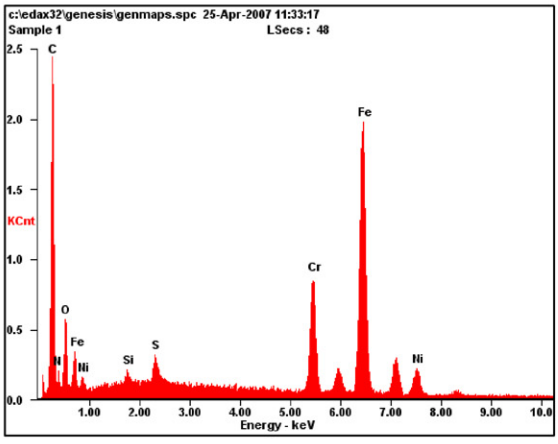

Element	Wt%	At%
CK	41.35	69.91
NK	04.22	06.12
OK	03.98	05.05
SiK	00.42	00.30
SK	01.02	00.65
CrK	08.87	03.46
FeK	35.03	12.74
NiK	05.12	01.77
Matrix	Correction	ZAF

Fig. 3. SEM and EDX after 10-h potentiostatic tests in the simulated anode and cathode environments of PEM fuel cells (a) anode (b) cathode.

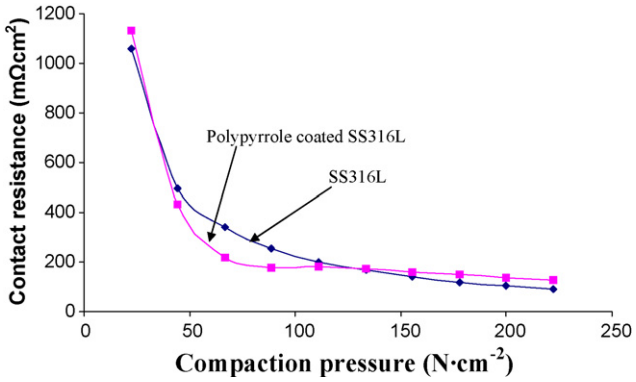

Fig. 4. Interfacial contact resistances for SS316L and polypyrrole-coated SS316L.

It is generally considered that PEM fuel cells should have operating lifetimes over 5000 h for transportation applications [21]. If the corrosion rate remains the same for the 5000 h lifetime of the fuel cell, Fe, Cr, Ni, Mn ion concentrations will reach 375 ppm, 65 ppm, 40 ppm, 9 ppm at the anode, and 613 ppm, 115 ppm, 90 ppm, 18 ppm at the cathode after 5000 h for uncoated SS316L. Fe, Cr, Ni, Mn metal ion concentrations will reach 147 ppm, 29 ppm, 25 ppm, 5 ppm at the anode, and 318 ppm, 30 ppm, 46 ppm, 9 ppm at the cathode after 5000 h for polypyrrole-coated SS316L. Let us suppose that 5% percent of metal ions remain in solution, and then the total metal concentrations are 25 ppm and 42 ppm at the anode and cathode for uncoated SS316L, respectively, and 10 ppm at the anode and 20 ppm at the cathode, respectively, after 5000 h for polypyrrole-coated SS316L. Although such levels of metal ion concentration are still too high for satisfactory PEM fuel cell performance for the uncoated SS316L, they are approaching satisfactory levels for the polypyrrole-coated SS316L.

We have earlier shown that the metal ion concentration after potentiostatic testing can be significantly decreased through the use of an Au-interlayer between the SS316L base material and the polypyrrole coating [22].

3.6. Contact resistance tests

Fig. 4 shows the variation of contact resistance of SS316L and polypyrrole-coated SS316L with compaction pressure. The polypyrrole coating (condition 5) was chosen for the contact resistance tests in order to be consistent with the corrosion tests. Also, we have found that the contact resistance does not change significantly when we change the coating thickness. With increasing compaction pressure from 20 N cm^{-2} to 220 N cm^{-2}, the contact resistance decreased rapidly at low compaction pressures and then decreased gradually, probably due to a decrease in interfacial resistance [23]. Comparing the two curves, we can see that the contact resistance of polypyrrole-coated SS316L is lower than that of SS316L from 20 N cm^{-2} to 130 N cm^{-2}, and then contact resistance of polypyrrole-coated SS316L become slightly higher than that of SS316L from 130 N cm^{-2} to 220 N cm^{-2}. The basic finding is that the contact resistance of SS316L is only changed slightly after coating with polypyrrole. This is probably because of the good electrical conductivity of the polypyrrole coating. We can know that the polypyrrole coating has good electrical conductivity from the SEM pictures. When we did the SEM test for the polypyrrole-coated SS316L, we do not need coat a thin layer gold on the sample surface to increase its electrical conductivity.

4. Conclusions

A Taguchi DOE method was used to optimize the polypyrrole-coating parameters for SS316L for metallic bipolar plate application. The potentiodynamic and SEM test results have shown that the relatively thick polypyrrole coatings can provide good corrosion resistance, with corrosion rates being decreased about 10 times relative to uncoated samples. In the simulated anode conditions of a PEM fuel cell, the corrosion current for polypyrrole-coated SS316L is negative, which can provide partial protection for the metal. In the simulated cathode conditions of a PEM fuel cell, the corrosion current is positive. Therefore, the corrosion was more severe at the cathode. From the ICP-OES test results, we found that the total metal ion concentrations were 25 ppm and 42 ppm at the anode and cathode, respectively, for uncoated SS316L, and 10 ppm and 20 ppm at the anode and cathode, respectively, for polypyrrole-coated SS316L. This is approaching the target of 10 ppm (total metal ion concentration) for the 5000 h lifetime of a PEM fuel cell. Also the contact resistance of SS316L with carbon paper does not change significantly after coating with polypyrrole.

Acknowledgements

The research was financially supported by the Natural Sciences and Engineering Research Council of Canada (NSERC) through a Discovery Grant awarded to Prof. D.O. Northwood. Yan Wang would like to acknowledge financial support through an Ontario Graduate Scholarship.

References

[1] A. Hermann, T. Chaudhuri, P. Spagnol, Int. Hydrogen Energy 30 (2005) 1297–1302.
[2] H. Tsuchiya, O. Kobayashi, Int. J. Hydrogen Energy 29 (2004) 985–990.
[3] M.J. Kelly, G. Fafilek, J.O. Besenhard, H. Kronberger, G.E. Nauer, J. Power Sources 145 (2005) 249–252.
[4] T. Okada, Y. Ayato, M. Yuasa, I. Sekine, J. Phys. Chem. B 103 (1999) 3315–3322.
[5] Y. Wang, D.O. Northwood, Adv. Mater. Res. 41–42 (2008) 469–475.
[6] S. Joseph, J.C. McClure, R. Chianelli, P. Pich, P.J. Sebastian, Int. J. Hydrogen Energy 30 (2005) 1339–1344.
[7] M.A. Lucio García, M.A. Smit, J. Power Sources 158 (2006) 397–402.
[8] Y. Wang, D.O. Northwood, J. Power Sources 163 (2006) 500–508.
[9] P.J. Ross, Taguchi Techniques for Quality Engineering, McGraw-Hill International Editions, USA, 1988.
[10] Y. Wang, D.O. Northwood, Optimization of the Polypyrrole-coating Parameters for PEM Fuel Cell Bipolar Plates using the Taguchi Method Corrosion Control 007, Sydney, Australia, November 25–28, 2007.
[11] Y. Wang, D.O. Northwood, Electrochim. Acta 52 (2007) 6793–6798.
[12] G. Hoogers, Fuel Cell Technology Handbook, CRC Press LLC, 2003, pp. 1–4.
[13] H. Wang, M.A. Sweikart, J.A. Turner, J. Power Sources 115 (2003) 243–257.
[14] D.P. Davies, P.L. Adcock, M. Turpin, S.J. Rowen, J. Appl. Electrochem. 30 (2000) 101–105.
[15] Y. Wang, D.O. Northwood, An investigation into the nucleation and growth of an electropolymerized polypyrrole coating on a 316L stainless steel surface, Thin Solid Films, in press.
[16] D.A. Jones, Principles and Prevention of Corrosion, 1st ed., Macmillan, New York, 1992, p. 147.
[17] Y. Wang, D.O. Northwood, J. Power Sources 165 (2007) 293–298.
[18] Y. Wang, D.O. Northwood, Int. J. Hydrogen Energy 32 (2007) 895–902.
[19] L. Ma, S. Warthesen, D.A. Shores, J. New Mater. Electrochem. Syst. 3 (2000) 221–228.
[20] M.P. Brady, K. Weisbrod, I. Paulauskas, R.A. Buchanan, K.L. More, H. Wang, M. Wilson, F. Garzon, L.R. Walker, Scripta Mater. 50 (2004) 1017–1022.
[21] R.G. Rajendran, MRS Bull. 30 (2005) 587–590.
[22] Y. Wang, D.O. Northwood, J. Power Sources 175 (2008) 40–48.
[23] E.A. Cho, U.S. Jeon, S.A. Hong, I.H. Oh, S.G. Kang, J. Power Sources 142 (2005) 177–183.